Unusual field dependence of remanent magnetization in granular CrO_2: the possible relevance of piezomagnetism

2010 J. Phys.: Condens. Matter 22 096005

(http://iopscience.iop.org/0953-8984/22/9/096005)

J. Phys.: Condens. Matter **22** (2010) 096005 (6pp) doi:10.1088/0953-8984/22/9/096005

Unusual field dependence of remanent magnetization in granular CrO_2: the possible relevance of piezomagnetism

A Bajpai[1], R Klingeler[1], N Wizent[1], A K Nigam[2], S-W Cheong[3] and B Büchner[1]

[1] Leibniz-Institute for Solid State and Materials Research, IFW Dresden, D-01171 Dresden, Germany
[2] Department of Condensed Matter Physics and Material Science, Tata Institute of Fundamental Research, Homi Bhabha Road, Mumbai 400 005, India
[3] Rutgers Center for Emergent Materials and Department of Physics and Astronomy, Rutgers University, Piscataway, NJ 08854, USA

Received 17 September 2009, in final form 21 December 2009
Published 10 February 2010
Online at stacks.iop.org/JPhysCM/22/096005

Abstract
We present low field thermoremanent magnetization (TRM) measurements in granular CrO_2 and composites of ferromagnetic (FM) CrO_2 and antiferromagnetic (AFM) Cr_2O_3. TRM in these samples is seen to display two distinct timescales. A quasi-static part of remanence, appearing only in the low field regime, exhibits a peculiar field dependence. TRM is seen to first rise and then fall with increasing cooling fields, eventually vanishing above a critical field. Similar features in TRM have previously been observed in some antiferromagnets that exhibit the phenomenon of piezomagnetism. Scaling analysis of the TRM data suggest that presumably piezomoments generated in the AFM component drive the FM magnetization dynamics in these granular systems in the low field regime.

(Some figures in this article are in colour only in the electronic version)

1. Introduction

For granular specimens of half-metallic ferromagnet CrO_2 ($T_C \approx 393$ K), it has been demonstrated earlier that the growth of an insulating oxide Cr_2O_3 naturally occurs on the surface of the CrO_2 grains [1–4]. This makes granular CrO_2 an attractive magnetoresistive material that exhibits spin-polarized tunnelling through the network of metallic grains of CrO_2, separated by an insulating grain boundary of Cr_2O_3 [1–3]. This also gives the system a very interesting aspect: a spin-polarized metal in contact with a dielectric. It is to be noted that the dielectric under consideration (i.e. Cr_2O_3) in its bulk form is a well-known room temperature AFM ($T_N \approx 307$ K) and a prototypical magnetoelectric material [5–8]. However, the manner in which its AFM character affects the magnetic and transport properties, when it appears as a grain boundary in granular CrO_2, remains largely unexplored. The primary difficulty arises due to the fact that it is hard to track the subtle change in the AFM grain boundary in the presence of strongly ferromagnetic CrO_2, at least through routine magnetization measurements.

A possible means of disentangling the magnetic contribution from FM CrO_2 and AFM Cr_2O_3 is to perform thermoremanent magnetization measurements. A study of remanent magnetization (via cooling a magnetic system through its transition temperature under a fixed magnetic field) reveals important information regarding domain motion, pinning mechanisms and other metastable states. The efficiency of these measurements in probing antiferromagnets has been demonstrated earlier [9–13].

2. Experimental details

We investigate granular CrO_2 in which Cr_2O_3 appears as a grain boundary, and highly diluted composites of CrO_2 and Cr_2O_3 with varying mass fraction of Cr_2O_3. These sintered pellets have CrO_2 grains in the shape of large micron-sized rods (5–10 μm length) [14, 15]. Figures 1(a) and (b) are

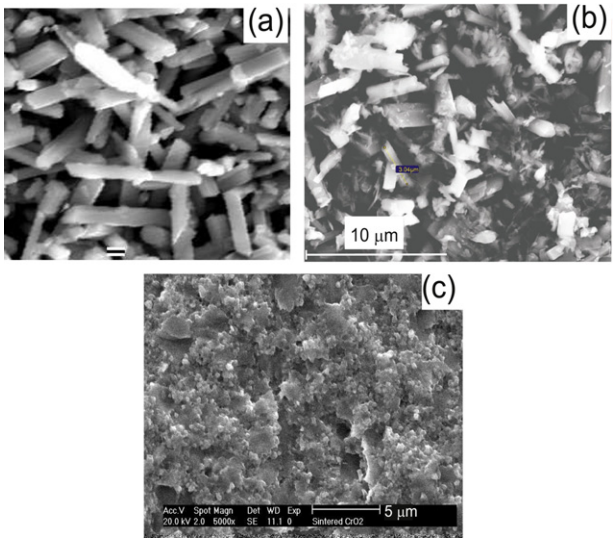

Figure 1. Scanning electron micrographs for CrO_2 samples containing (a) 10%, (b) 40% and (c) 75% mass fraction of Cr_2O_3. In (a) and (b), the long micron-sized rods of CrO_2 grains are visible. (c) On further annealing under high pressure, the grains are seen to coagulate.

the scanning electron micrograph pictures of the sintered pellets, which contain about 10% and 40% mass fraction of Cr_2O_3, respectively. On the individual CrO_2 grains (rod-like micro-crystals), the AFM oxide Cr_2O_3 appears as a surface layer (or grain boundary). In this microstructural regime, the samples mimic a typical 'metal-in-insulator scenario' which has also been observed in compacted commercial powders of CrO_2 [2, 3]. These samples can be termed as 'granular metals' as far as their electron transport properties are concerned [2, 16]. We also investigate a sample which is further sintered under high pressure (6 GPa) and high temperature (up to 700 °C). The process of high pressure annealing results in a composite with 75% mass fraction of Cr_2O_3 and more importantly the coagulation of CrO_2 grains (figure 1(c)). Magnetization measurements on all these samples are done using a Quantum Design SQUID magnetometer.

3. Magnetization measurements

As mentioned earlier, the *activated* transport observed in the resistivity of granular CrO_2 clearly manifests the influence of the insulating grain boundary [1–3]. In our samples with micron-sized rods of CrO_2, many new features in magnetotransport were unravelled which are seen to be in tune with the grain boundary density [14, 16]. For instance, unlike commercial powders, we see two distinct regions in 'activated transport', a significantly enhanced magnetoresistance and experimental signatures suggesting that the magnetism of the grain boundary influences the magnetotransport [16, 17]. However, it is difficult to probe the grain boundary magnetism since both the field ($M(H)$) and temperature dependence of magnetization ($M(T)$) follows a classical ferromagnetic behaviour arising from CrO_2, thus remaining insensitive to the presence of AFM Cr_2O_3 [16]. Some key magnetization measurements are summarized in figure 2. Figure 2(a) displays an MH isotherm measured at 5 K for the sample with 10% mass fraction of Cr_2O_3. The saturation magnetization (M_S) value at 1 T is of the order of 120 emu g^{-1} (or 1.85 μ_β/Cr ion) for the ferromagnetic phase. The shape of the $M(H)$ isotherm is qualitatively similar to what is seen in the epitaxial thin films of CrO_2, which exhibit nearly perfect saturation magnetization ($M_S \approx 135$ emu g^{-1} at 1 T, corresponding to 2 μ_β/Cr ion) and very small opening of the loop [18]. The inset in figure 2(a) shows the $M(H)$ isotherms measured at 5 K for samples with 40 and 75% mass fraction of Cr_2O_3. It is evident that increasing the mass fraction of Cr_2O_3 results in a systematic reduction of M_S but the shape of the $M(H)$ isotherm and other parameters such as coercivity remain similar to what is seen in the 10% sample. The minor hysteresis loop traced up to the field of 1.5 kOe shows that even in the zero-field-cooled protocol, the $M(H)$ isotherm exhibits an asymmetric loop with low coercivity field values, $H_C \approx 50$ Oe and remanent magnetization of 2–5 emu g^{-1} (figure 2(b)). It is also observed that $M(T)$ scans measured in low field exhibit field-cooled (FC) and zero-field-cooled (ZFC) bifurcation, which vanishes when the applied field is more than 500 Oe, as is shown in figure 2(c) for the temperature range between 300 and 450 K. Similar history effects are observed in $M(T)$ scans measured between 5 and 350 K. Figure 2(d) shows $M(T)$ scans measured in the FC state at various fields for the sample with 40% Cr_2O_3. Here, the magnetization is also seen to increase with increasing magnetic field and eventually saturates for fields of the order of 1 T. Similar traits are exhibited by two other samples used in this work.

4. The thermoremanent magnetization measurements

In figure 3, we display TRM measurements for all three samples. The protocol of the TRM measurements is as follows: the sample is cooled from 350 to 5 K in the presence of a fixed magnetic field, hereby referred to as H_{cool}. At 5 K, the field is switched off and the remanent magnetization is recorded as a function of temperature in heating cycles. We emphasize that, as soon as the magnetic field is switched off, the magnetization is seen to decay almost instantly with time. However, it eventually arrives at some residual value where it stays without a notable decay. For instance, we take note from figure 2(d) of the 'infield' magnetization value for the 40% composite, which is around 15 emu g^{-1} at 5 K at a measuring field of 100 Oe. On switching off the field at 5 K, the magnetization attains a residual value of about 5 emu g^{-1} (figure 3(b)). This 'residual' remanent magnetization is fairly long lived in the experimental timescale. What we have plotted in figure 3 is the temperature variation of this quasi-static remanence, measured for various H_{cool}.

Figure 3(a) displays temperature variation of TRM on the sample with 10% mass fraction of Cr_2O_3, for a few selected values of H_{cool}. The magnitude of TRM first increases with increasing H_{cool} and attains its maximum value at a critical cooling field. Above this field, the TRM is seen to decrease

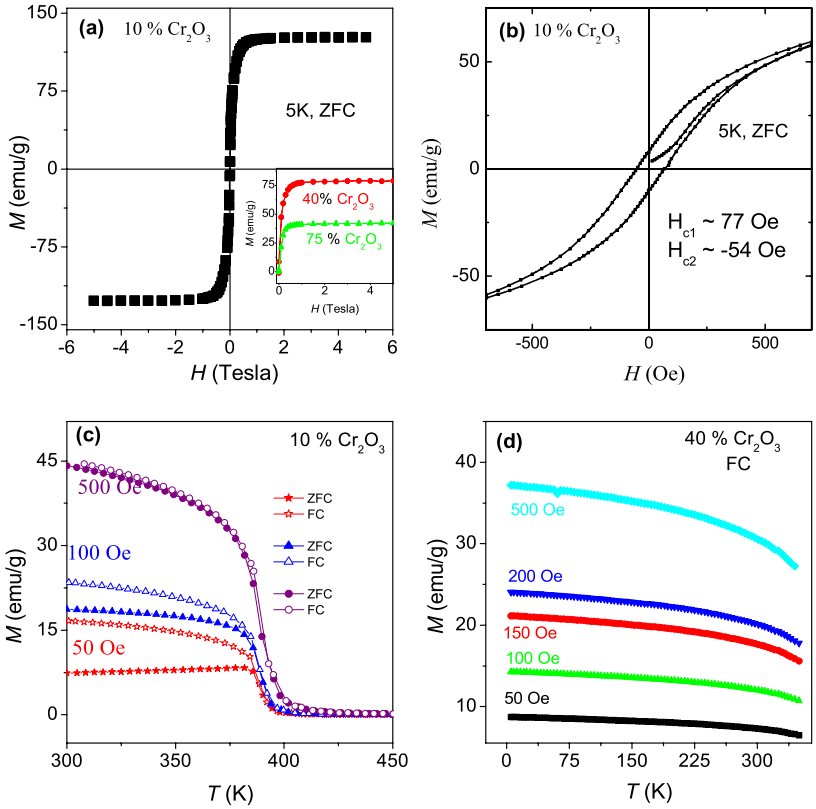

Figure 2. (a) $M(H)$ isotherm recorded at 5 K in the ZFC state for CrO_2 sample with 10% (main panel), 40% and 75% mass fraction of Cr_2O_3 (lower inset). (b) Minor $M(H)$ loop at 5 K, traced in the ZFC state for the sample with 10% Cr_2O_3, exhibiting slightly asymmetric H_C. (c) Magnetization as a function of temperature in various magnetic fields. Low field magnetization exhibits history effects (FC and ZFC bifurcation) which vanish when the applied field is above 500 Oe. (d) Magnetization as a function of temperature in various magnetic fields between 50 and 500 Oe for the sample with 40% mass fraction of Cr_2O_3. The sample is field-cooled down to 5 K; subsequently data is recorded in the heating cycle in the presence of the field.

in magnitude with increasing H_{cool} and eventually vanishes at cooling fields of about 1 kOe. For all our measurements, the residual field of the SQUID magnetometer (which is estimated to be of the order of 2–5 Oe during the measurement) is not seen to interfere with this unusual field dependence of TRM. For the same sample, we also conducted TRM measurements in the high temperature oven in the SQUID magnetometer so as to heat the sample above 400 K (T_C of the FM grain) after each measurement. This dataset is displayed in the inset of figure 3(a). Here the H_{cool} was applied at 450 K which is much above the T_C of the FM grain and the T_N of the AFM grain boundary. Subsequently, the sample is cooled down to 300 K and the TRM is measured as described earlier. The TRM and its unusual field dependence is seen to persist right up to 400 K, the T_C of FM CrO_2. Qualitatively similar features are observed when the direction of H_{cool} is reversed.

These experimental signatures are reproduced in composites of CrO_2/Cr_2O_3, irrespective of the mass fraction of Cr_2O_3 or the microstructure, as is evident from figures 3(b) and (c). Figure 3(b) displays the TRM measured in negative cooling fields for a composite containing 40% mass fraction of Cr_2O_3. The grain size of CrO_2 in this sample was similar to the sample with 10% mass fraction of Cr_2O_3. Figure 3(c) displays the symmetric nature of TRM in positive and negative cooling fields for the 75% composite. The unusual field dependence of TRM is clearly depicted in the inset of figure 3(c) where the TRM at 5 K is plotted against the H_{cool} from the cross section of various temperature scans for the 75% composite. We emphasize that the unusual field dependence of TRM (inset of figure 3(c)) is qualitatively similar to what is seen in the other two samples. However the field at which the TRM reaches its maximum, and also the field at which it vanishes, varies slightly from sample to sample. Also, as is evident from figures 2(c) and (d), for low applied fields, the magnetization value and therefore the magnitude of the TRM depends on the field and thermal history of the sample. However, the key features including the observation of the quasi-static remanence as well as its unusual field dependence (inset of figure 3(c)) are reproduced irrespective of the field and thermal history prior to the measurement of TRM. The TRM data obtained on a variety of samples indicate that the peculiar field dependence of TRM is intrinsic to these materials. More importantly, it appears only in the low field limit.

The unusual field dependence of TRM is not reflected in the routine 'in-field' magnetization in any of these samples, as can be seen in figure 2. In all these samples, the magnetization increases in magnitude with increasing applied field (figure 2(d)) and saturates at about 1 T (figure 2(a)), consistent with FM CrO_2 [16]. Thus it is clear that, while regular M versus T data exhibit no surprises, for the

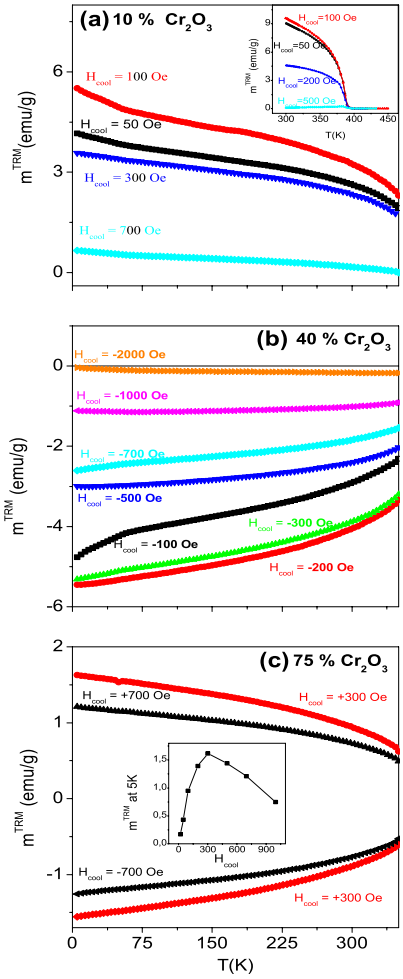

Figure 3. (a) TRM as a function of temperature for CrO_2 samples containing (a) 10%, (b) 40% and (c) 75% mass fraction of Cr_2O_3 in various H_{cool}. The inset in (a) shows the same for the temperatures between 300 and 450 K for the 10% sample. The inset in (c) shows TRM values at 5 K plotted as a function of H_{cool} for the sample with 75% mass fraction of Cr_2O_3.

similar measurement protocol, a part of TRM exhibits an unusual field dependence. This field dependence of TRM is strikingly different from what is usually seen in TRM arising in magnetic systems including granular ferromagnets [19], diluted antiferromagnets or spin glasses [9, 20]. For instance, in these systems, TRM is often seen to rise with increasing magnetic field and eventually saturates above a critical field [19, 20]. However, observation of a peak effect as well as the vanishing of TRM at such low fields is unprecedented. We also note that neither the peak nor the vanishing of the TRM occurs at a field which matches with the coercivity of CrO_2. As can be seen from figures 2(a) and (b), the coercivities are in the range of 50–70 Oe when the $M(H)$ isotherm is traced in the ZFC state. We also checked the coercivities in the field-cooled state and they also show an asymmetric loop similar to figure 2(b), with coercivities still in the range of 50–70 Oe (not shown here). It is clear that a part of the remanence, which exhibits instant decay after switching off the field, arises from the regular domain wall dynamics intrinsic to FM CrO_2. However, the quasi-static remanence appears to be intimately connected to the magnetization at the AFM/FM interface.

4.1. Origin of quasi-static remanence and related pinning mechanism

A possible scenario is that the AFM phase pins the FM spins at the interface related to an unusual pinning mechanism giving rise to this quasi-static remanence. However, this pinning does not seem to appear from conventional exchange bias alone. Though exchange bias is certainly expected at the FM/AFM interface this contribution to TRM should have vanished around 300 K (near the T_N of Cr_2O_3). Moreover, the exchange bias field is inversely proportional to the magnetization of the FM layer [21]. It is evident that, within this simplistic picture, the peak in TRM at moderate fields of the order of 100–200 Oe and also the vanishing of TRM at fields of the order of 1–2 kOe cannot be understood. Thus, though exchange bias effects at the FM/AFM interface may be present, the observed TRM and the related pinning mechanism does not seem to arise from it. We also recall that a spin flop phase in Cr_2O_3 is known to occur at fields of the order of 5.8 T and temperatures below 90 K [8]. However, the unusual field dependence of TRM (in a wide temperature range between 5 and 400 K) cannot be understood by invoking spin flop in the AFM layer. Besides the fact that a field-induced spin flop transition is extremely unlikely at such moderate fields, neither the field dependence nor the vanishing of TRM can be explained by this scenario.

It is important to recall that similar features in TRM, especially in the low field regime, have been previously observed in certain AFMs [9–13]. In the case of $FeZnF_2$ [9] and epitaxial thin films of Cr_2O_3 [13], these features are understood to arise from piezomagnetically [22] frozen moments. Here, piezomagnetism is defined as a third rank tensor (P_{ijk}) relating the component of magnetization (M_i) induced in the 'i' direction due to the applied stress σ_{jk} ($M_i = P_{ijk}\sigma_{jk}$) [23]. This phenomenon, based on crystal symmetry considerations, was first predicted for rutile antiferromagnets [22]. For rhombohedral AFMs such as α-Fe_2O_3 and Cr_2O_3, the piezomagnetic coefficients P_{ijk} have been deduced from the single-ion magnetoelastic tensor. While this theory predicts finite P_{ijk} for Fe_2O_3, the net piezomoment was estimated to be zero for bulk Cr_2O_3 [23]. It remains to be verified whether these predictions are also valid for thin films of Cr_2O_3, after taking into account the altered symmetry conditions at the interface. However, there has been a recent theoretical estimation of a piezomagnetic tensor, which is independent of the crystal symmetry considerations as well as of the magnetic state of the sample. These calculation are relevant when a bulk shear wave is propagating at the interface of a semibounded dielectric [26]. It has also been suggested that a small but finite piezomagnetoelectric effect can arise in rhombohedral Cr_2O_3 as a consequence of the symmetry of its magnetic point group [24, 25]. In our samples, where Cr_2O_3 appears as a surface layer outside the FM CrO_2, the situation is conducive for the observation of such effects as Cr_2O_3, which is intrinsically a magnetoelectric compound subjected to both the natural stress due to the lattice mismatch and the internal field of the FM grain at the interface. We also emphasize that, owing to the fact that the FM grain is metallic whereas the surface layer is insulating, the stress effect should

further enhance during thermal cycling, due to widely different thermal conductivities of its individual components.

In our CrO_2/Cr_2O_3 samples, we note that the TRM vanishes only above 390 K which is the actual FM T_C, thus indicating that it primarily arises from the ferromagnetic grains. However, qualitative features of TRM, particularly its field dependence, are remarkably similar to the TRM data obtained on thin films of AFM Cr_2O_3 [13]. This correlation strongly suggests that at least low field TRM in our samples is modulated by the grain boundary and gives rise to an unconventional pinning mechanism at the FM/AFM interface. It appears that, in the low field regime, this pinning may arise exclusively due to the piezomoments generated in the AFM Cr_2O_3. These piezomoments can arise due to the natural stress at the interface coming from the lattice mismatch between rutile CrO_2 ($a = 4.42$ Å, $c = 2.92$ Å) and rhombohedral Cr_2O_3 ($a = 4.95$ Å, $c = 13.59$ Å). As in the case of thin films of pure Cr_2O_3, these effects appear to peak and saturate in a moderate field range of a few 100 Oe. It has been shown in films of Cr_2O_3 that the pinned moment follows similar field dependence (first increasing with increasing field and then saturating at a few 100 Oe) even above the T_N though the magnitude of this effect is smaller [13] as compared to what we observe in our samples.

The generation of finite piezomoment in the epitaxial thin films of pure Cr_2O_3 has been concluded from both the functional form as well as the observation of a scaling behaviour in TRM. Such scaling is understood to arise from the factorization of the piezomoment, due to which magnetization is a product function of field and temperature according to the equation $m(H,T) = f(H)g(T)$, where f and g are functions of field and temperature [13]. Scaling is achieved by normalization of the moment to its value at any fixed temperature which is less than T_N. Interestingly, we also find that TRM data recorded at various H_{cool}, when normalized by TRM at any temperature above 200 K, fall into a single curve. Figure 4 displays TRM normalized to its value measured at 300 K for the sample with 10% mass fraction of Cr_2O_3. The inset shows the scaling for the TRM measured between 5 and 350 K for the same sample. Here the normalization is done with a TRM value measured at 240 K. Deviations from the scaling are observed for H_{cool} more than 200–300 Oe or when TRM is normalized with its value below 200 K. Observation of the scaling in this field and temperature window also indicates that possibly similar piezomagnetic traits of AFM Cr_2O_3 leads to the unusual magnetization dynamics in granular CrO_2.

Once pinned from the process of field cooling through the T_N (307 K) of Cr_2O_3, the TRM is retained right up to 390 K, and also preserves its peculiar field dependence much above the T_N of Cr_2O_3 as is evident from the inset of figure 3(a). It appears that the unusual pinning mechanism which closely resembles the behaviour of pure Cr_2O_3 does not diminish even above the T_N of Cr_2O_3. In this context, we recall that there have been other experimental evidence in some FM/AFM systems which have shown unusual exchange bias effects at temperatures above the T_N of the AFM component. These effects are attributed either to a strain or proximity effect [27]. For instance, trilayer $Fe/Cr_2O_3/Fe$ structures have

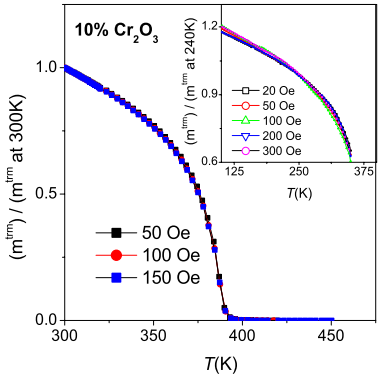

Figure 4. The main panel shows normalized TRM in the temperature range between 300 and 450 K exhibiting a scaling behaviour in various cooling fields, H_{cool}. The inset shows the normalized TRM for dataset recorded between 5 and 350 K. It is seen that, for lower H_{cool}, when normalized with any temperature above 200 K, the data collapse into a single curve.

shown unusual exchange bias effects right up to 395 K. In the case of pure Cr_2O_3, the atomic magnetoelectric coefficient may exist in the paramagnetic regime but the net effect enhances when long range AFM order sets in [7]. On similar lines, a possible scenario is that, in low fields, while cooling through the T_N of Cr_2O_3, the pinned moment at the FM/AFM interface is driven by additional stress-induced moments intrinsic to the AFM component. Once frozen, these pinned moments remain intact during heating even above the T_N, as the stress due to the lattice mismatch will still be finite. However, larger fields lead to the pinning of the FM moment according to the interplay between the direction of the field and the anisotropy of the FM component. This part of the remanence is not quasi-static and decays instantaneously on removal of the field. This is also consistent with the vanishing of TRM when the applied field is larger, as the quasi-static remanence (if related to the piezomagnetic effect) is a weak effect and is washed off in higher fields. This picture is also consistent with the fact that the peak in TRM and the vanishing of TRM does not relate to the coercivity of the FM component. However, it appears to be intimately connected to the field dependence of the stressed films of pure Cr_2O_3 and also other antiferromagnets which have shown such quasi-static remanence. Thus low field magnetization data indicate the possible relevance of piezomagnetic effects. The appearance of quasi-static remanence and its peculiar field dependence conveys that the stress effects need to be explored carefully in granular CrO_2.

The quasi-static remanence appearing in low fields can have interesting implications as the magnitude of the pinned moment is significantly large, unlike what is seen in epitaxial thin films of Cr_2O_3. For samples with similar grain size of CrO_2, we note that the magnitude of TRM does not vary significantly with increasing mass fraction of Cr_2O_3, indicating that the pinned moment is related to the CrO_2/Cr_2O_3 interface. We expect that decreasing the grain size would lead to enhanced magnitude of the pinned moment at the FM/AFM interface. Recently some computational studies, which take into account the altered symmetry conditions at the

interface of two dissimilar materials, indicate unconventional magnetoelectric effects [28]. Similar theoretical investigations are needed to address the issues related to piezomagnetism in Cr_2O_3, especially when it appears at the interface.

5. Conclusions

In conclusion we present low field thermoremanent magnetization data on the composites of CrO_2/Cr_2O_3. This measurement spectacularly brings out that the effects of magnetization of the AFM part, which is not visible in routine 'in-field' magnetization in the granular CrO_2 sample. The data also indicate that presumably the stress effects, which can naturally occur at the interface of this spin-polarized metal (CrO_2) and magnetoelectric insulator (Cr_2O_3) due to the lattice mismatch, may give rise to a finite piezomoment in Cr_2O_3. This, in the low field limit, modulates the magnetization of CrO_2. Once frozen from the process of field cooling, these piezomoments can pin the magnetization of FM spins at the interface and thus open up additional possibilities of tuning the spintronic devices via stress-mediated coupling in granular CrO_2.

Acknowledgments

AB acknowledges support through the EU Marie Curie IIF Fellowship under project 040127-NEWMATCR. Work at Rutgers was supported by NSF-DMR-0804109.

References

[1] Hwang H Y and Cheong S-W 1997 *Science* **278** 1607
[2] Coey J M D, Berkowitz A E, Balcells L and Putris F F 1998 *Phys. Rev. Lett.* **80** 3815
[3] Dai J *et al* 2000 *Appl. Phys. Lett.* **77** 2840
[4] Dai J and Tang J 2001 *Phys. Rev.* B **63** 054434
[5] Rado G T and Folen V J 1961 *Phys. Rev. Lett.* **7** 310
[6] Folen V J, Rado G T and Stalder E W 1961 *Phys. Rev. Lett.* **6** 607
[7] Martin T J and Anderson J C 1964 *Phys. Lett.* **11** 109
[8] Fiebig M, Froehlich D and Thiele H J 1996 *Phys. Rev. Lett.* **54** 2681
[9] Kushauer J, Kleemann W, Mattsson J and Nordblad P 1994 *Phys. Rev.* B **49** 6346
[10] Palacio F, Gabas M, Campo J, Becerra C C, Paduan Filho A P, Fries T and Shapira Y 1994 *Phys. Scr.* T **55** 163
[11] Mattsson J, Djurberg C and Nordblad P 2000 *Phys. Rev.* **61** 11274
[12] Fries T, Shapira Y, Paduan Filho A, Becerra C C and Palacio F 1993 *J. Phys.: Condens. Matter* **5** L07
[13] Sahoo S and Binek Ch 2007 *Phil. Mag. Lett.* **87** 259
[14] Bajpai A and Nigam A K *US Patent* 7276226
[15] Bajpai A and Nigam A K 2005 *Appl. Phys. Lett.* **87** 222502
[16] Bajpai A and Nigam A K 2007 *Phys. Rev.* B **75** 064403
[17] Bajpai A and Nigam A K 2007 *J. Appl. Phys.* **101** 103911
[18] Spinu L, Srikanth H, Gupta A, Li X W and Xiao G 2000 *Phys. Rev.* B **62** 8931
[19] Neel L 1953 *Rev. Mod. Phys.* **25** 293
[20] Benitez M J, Petracic O, Salabas E L, Radu F, Tueysuez H, Schueth F and Zabel H 2008 *Phys. Rev. Lett.* **101** 097206
[21] Mieklejohn W H and Bean C P 1957 *Phys. Rev.* B **105** 904
[22] Borovik-Romanov A S 1960 *Sov. Phys.—JETP* **11** 786
[23] Phillips T G and White R L 1967 *Phys. Rev.* **162** 382
[24] Rado G T 1962 *Phys. Rev.* **128** 2546
[25] Grimmer H 1992 *Acta Crystallogr.* A **48** 266
[26] Shavrov V G, Lapteva T V and Tarasenko S V 2007 *Dokl. Phys.* **52** 527
[27] Sahoo S, Mukherjee T, Belashchenko K D and Binek Ch 2007 *Appl. Phys. Lett.* **91** 172506
[28] Rondinelli J M, Stengel M and Spaldin N 2008 *Nat. Nanotechnol.* **3** 46